The Physics of SERAPHIM

Barry Marder
Target and Z-pinch Theory
Sandia National Laboratories
P. O. Box 5800
Albuquerque, NM 87185-1186

Abstract

The Segmented Rail Phased Induction Motor (SERAPHIM) has been proposed as a propulsion method for urban maglev transit, advanced monorail, and other forms of high speed ground transportation. In this report we describe the technology, consider different designs, and examine its strengths and weaknesses.

Contents

Figures

The Physics of SERAPHIM

I. Introduction

Many proposals for a high speed ground transportation system (HSGT) have been advanced over the years. These range from simply improving conventional railroad technology, as with the French TGV [1], to high speed trains propelled, not by wheels, but by a linear induction motor (LIM) [2], to vehicles moving so fast that wheels are no longer an option and magnetic levitation (MAGLEV) is essential [3]. Of these three, the first is in daily service with an average speed of 186 mph (but capable of higher speed), the second has been built and tested to 250 mph in the 1970's, but never deployed, and the third has had many incarnations, some of which, propelled by a linear synchronous motor (LSM), have demonstrated speeds over 300 mph. This report describes a new propulsion technology which like LIMs and LSMs does not rely on wheel-track adhesion to provide thrust and may offer an attractive alternative.

For a HSGT system to be both safe and have minimal impact on the environment, it should be elevated along its entire length. It could follow existing highways or rail lines, and could cross farms, swamps, and forests with minimal adverse effect. For an elevated guideway to be inexpensive, however, both the structure and the loads its carries must be lightweight. This works against a conventional train, which must be heavy enough to maintain traction. To propel a lightweight vehicle at high speed, especially in bad weather and up steep grades, requires a means of propulsion that does not rely on wheel-track adhesion. With the LSM, proposed for most MAGLEV applications, the entire length of the guideway contains sensors, switches, and electromagnets which interact with a magnet (possibly superconducting) on the vehicle. Although costly and complex, LSMs are efficient and capable of very high speed. Because of projected reduced maintenance costs, MAGLEV is also being considered as an option for speeds below 200 mph. In this regime, however, wheels remain a viable option. If the vehicle is not levitated, the need to keep its weight down is somewhat mitigated so a powered motor, such as a LIM, can be placed on the vehicle, reducing the cost of the roadbed. The LIM guideway contains a conducting reaction rail against which the motor exerts an electromagnetic force.

As with any technology, LIMs have limitations. Its top speed is proportional to its length; the longer (and, thus, heavier) the motor is, the faster it can go. Its efficiency falls off sharply as this speed limit is approached. Also, because a LIM uses an iron core to shape and contain the magnetic fields, it works best when the gap between the motor poles and the reaction rail is small, requiring a high degree of precision in the guideway. SERAPHIM, the motor described in this report, represents an attempt to design an induction motor for which these restrictions are eased. This report describes the technology, show why it looks attractive, and address its weaknesses.

II. The original concept

Under the Strategic Defense Initiative, Sandia National Laboratories developed a novel, very high speed linear induction motor called a "coilgun" [4], designed to launch satellites from the ground with a velocity of 6 km/sec (13,500 mph, about 20 times the speed of sound)! A two meter long coilgun has launched projectiles at over 1 km/sec, demonstrating enough force to have accomplished the earth-to-orbit mission were the gun sufficiently long. To appreciate the magnitude of this force, consider that the coilgun achieved the average pressure exerted by a cannon. Of course, passenger vehicles are not intended to be "shot from guns", but when interest

in the earth-to-orbit launch waned, attention was focused on the possibility that a variation of this "star wars" motor could propel a high speed vehicle.

The force in coilguns arises from a gradient in mutual inductance between a powered primary coil and a passive armature in which current is induced. A simple example is a pair of nested solenoids, as illustrated in Figure 1. If the primary carries an alternating current, an opposite current will be induced in the shorted armature. The force between the two is the product of the currents times the gradient of the mutual inductance. Because the mutual inductance of the two solenoids is a maximum when they are together, and falls to near zero when they are far apart, an axial force is produced on the armature. In a coilgun, a sequence of thin, washer-like coils accelerated both aluminum cylinders and shorted solenoidal secondaries.
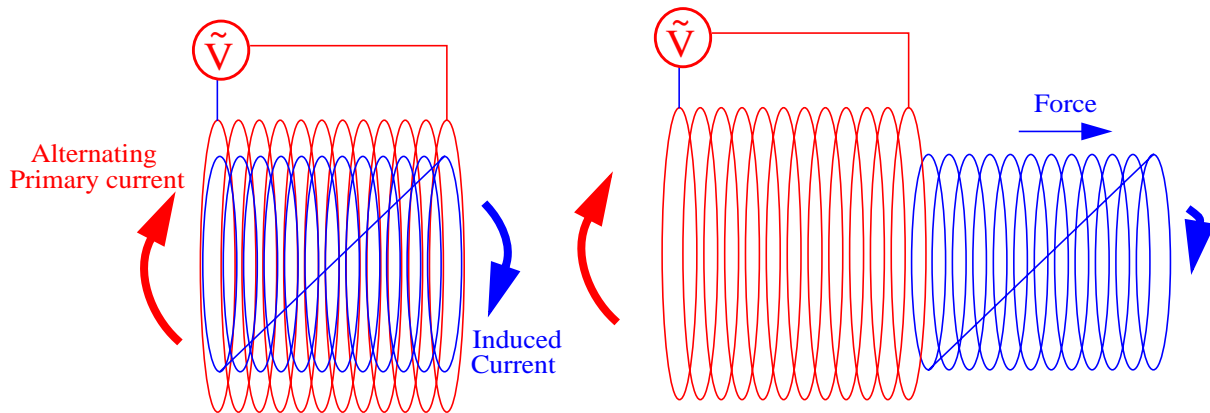

Figure 1. A dual-solenoid coilgun. The powered coil (red) induces a current in the shorted armature (blue), creating a force in the direction of diminishing mutual inductance.

There are many variations to this theme. The armature need not be a shorted winding, but could be a solid conducting cylindrical shell. Or, instead of coaxial solenoids, the launcher could consist of a "pancake" coil primary and a similar shorted armature, or solid plate, as in Figure 2.
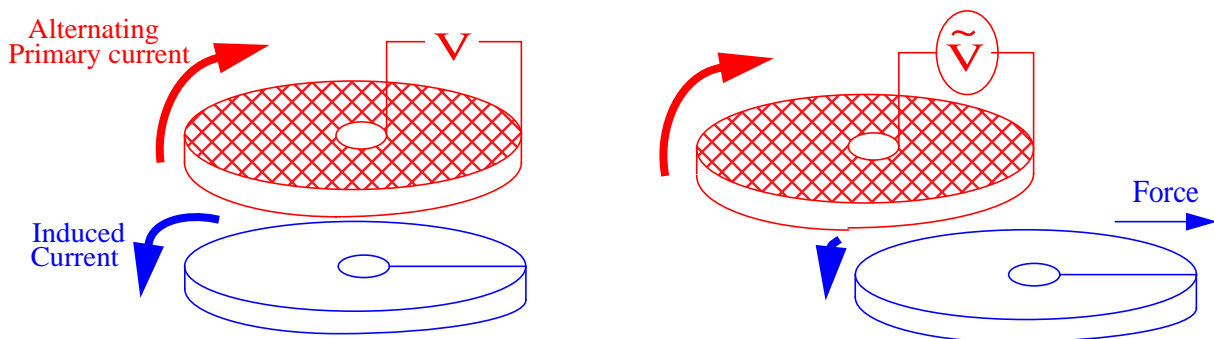

Figure 2. An inductive launcher using powered (red, cross hatched) "pancake" coils. The armature (blue) could be a shorted coil or a solid conducting plate.

The original Sandia launcher, called a "reconnection gun" [5], was of this second design. It accelerated a solid aluminum plate by passing it through a sequence of flat coils located on either side of a thin guideway. Each coil pair was connected to a charged capacitor and was switched on as the moving plate passed between them. The rising current in the coils induced currents in the plate, generating a force that pushed the plate away from the coil and accelerated it along the flyway.

If the roles of the plate and coils are reversed, the reconnection gun geometry looked attractive for vehicle propulsion. The powered pancake coils would be on the vehicle and they would straddle a succession of conducting plates on the roadbed. The plate position would again be sensed and the coils energized in such a manner as to expel them, providing thrust for the vehicle. Needing a catchy acronym, the concept was dubbed SERAPHIM, for Segmented Rail Phased Induction Motor [6]. A proof-of-principle demonstration was built and successfully tested with Department of Energy (DOE) funding, arising from dual-use national defense issues. Notice that, unlike a conventional LIM which generates eddy currents in a continuous reaction rail, this approach relies on the fact that the plate has an edge, for without the edge, there is no change in the mutual inductance as the armature moves past the powered coil.

III. The Dual Coil SERAPHIM

It became clear from our experience with the cylindrical coilgun, that a solid plate was not the best armature. The current path in a solid armature is not predetermined, as it is in wire. It depends, instead, on how the magnetic field diffuses through the metal which, in turn, is related to the resistivity and the drive frequency. Magnetic flux which has diffused into the metal can remain after the motor coil has moved on, representing an energy loss which adversely effects efficiency. Another, more serious, problem is the heating caused by concentrated current. In particular, a large, persistent current flows near the front edge, while the rear carries very little, as shown schematically in Figure 3. This can cause significant ohmic heating, or even melting!
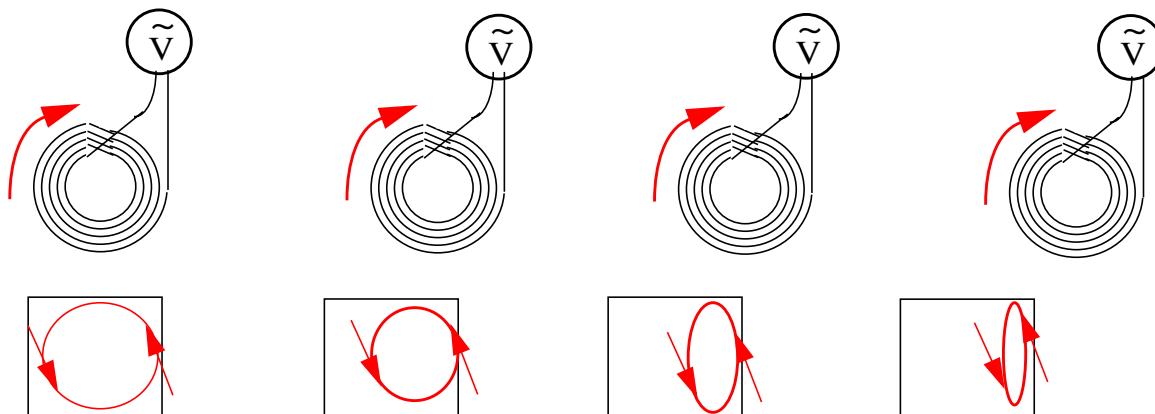

Figure 3. Symbolic representation of the alternating currents (red) in the moving powered coil (top) and solid armature plate (bottom). The armature actually lies under the drive coil. Note the persistent current concentration at the front edge of the plate.

If the reaction plate is replaced by a shorted coil similar to the powered one, as shown in Figure 4, many of the problems are resolved. The current now flows in wires so that classical electrical engineering methods can be used to model the behavior. With enough turns, the individual wires can be made sufficiently thin (less than or comparable to the skin depth), that little magnetic flux remains embedded in metal. Heating, both local and global, is less of a problem because the current density is nearly uniform throughout the entire coil.
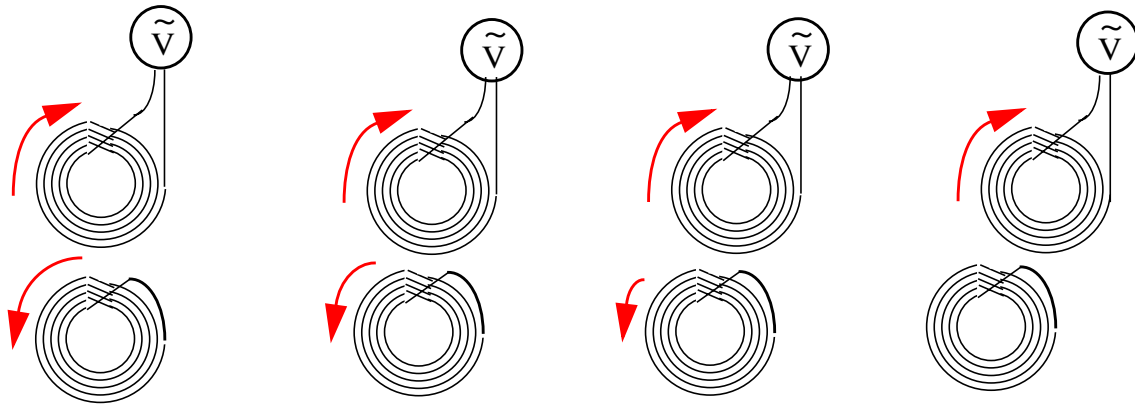
Figure 4. Dual coil design in which the stationary coil (bottom) is shorted. The mutual inductance vanishes when the coils are offset about half a radius, so no current is induced.

The electrical performance of the dual-coil SERAPHIM, is modeled numerically as two inductively coupled circuits. A coil is approximated by a resistor and inductor in series. Vehicle kinematics (motion) is included, but not dynamics (response). Both circular and rectangular coils can be analyzed. The geometry and circuits are shown in Figures 5 and 6.
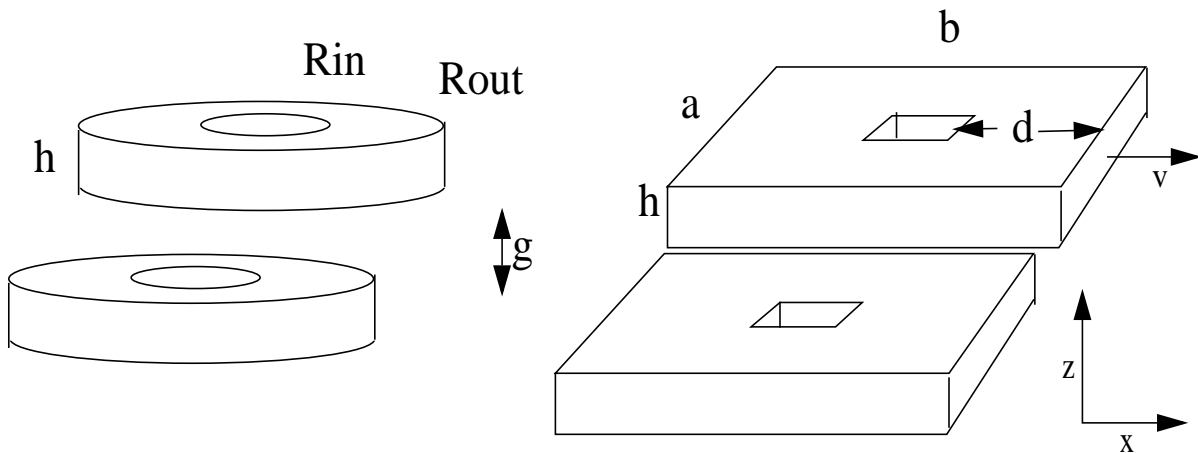

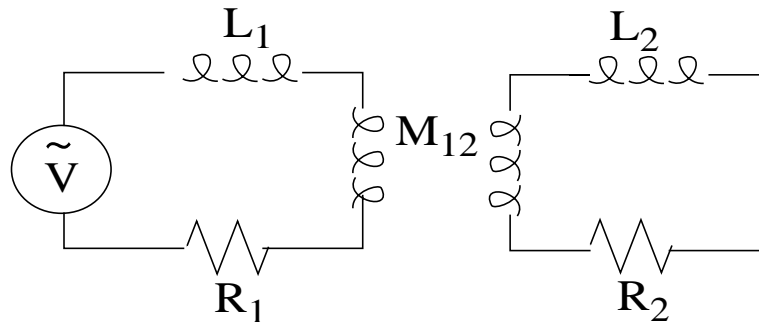*Figure 5. Circular (left) and rectangular (right) dual-coil geometries.*

Figure 6. Circuit for either the circular or rectangular dual-coil SERAPHIM. The rectangular winding width, d, is the same for both directions.

The equations for the drive current, I_1, and armature current, I_2, driven by a voltage, V_0, at frequency "f" are:

$$(1) \qquad L_1\frac{dI_1}{dt} + R_1I_1 + \frac{d}{dt}(M_{12}I_2) = V_0\cos\left(\frac{2\pi t}{f}\right)$$

$$(2) \qquad L_2\frac{dI_2}{dt} + R_2I_2 + \frac{d}{dt}(M_{21}I_1) = 0$$

The computation is typically started at peak voltage with the two coils located directly on top of each other and no current flowing in either. The coil resistances are determined from the resistivity of the coil material, its temperature, and geometry. A fill factor is included to account for insulation and support. The inductance calculations are described in Appendix 1. Resistances and self inductances are computed once at the start. Because the top coil moves, the mutual inductance is re-computed at each time step. Eqs. (1) and (2) are approximated as difference equations and solved numerically.

The forces in the direction of motion (thrust), x, and along the axis (lift), z, are:

$$(3) \qquad F_x = -I_1I_2\frac{\partial M_{12}}{\partial x} \qquad F_z = -I_1I_2\frac{\partial M_{12}}{\partial z}$$

The inductive energy and expended ohmic and kinetic energies are:

$$(4) \quad E_{IND} = \frac{1}{2}(L_1I_1^2 + L_2I_2^2) + M_{12}I_1I_2 \qquad E_{RES} = \int_0^t I_1^2R_1 + I_2^2R_2\,dt \qquad E_{KIN} = \int_0^t F_x v\,dt$$

Notice that the kinetic energy depends on the velocity. An efficiency, η, can be defined as

$$(5) \qquad \eta = \frac{E_{KIN}}{E_{IND} + E_{RES} + E_{KIN}}.$$

The inductive energy does not enter into the actual efficiency because switching is done at current nulls, when it vanishes. It does, however, play a significant role in designing a power supply, as the circulating inductive power can be substantial.

IV. Inductive behavior

As an example, consider a pair of square (b/a=1), thick build (d/a=0.5), coils with powered and passive coil heights related to their widths by $h_1/a = 0.08$ and $h_2/a = 0.05$ respectively. Much can be inferred about the behavior from the spatial dependence of the mutual inductance or, equivalently, the coupling coefficient, defined by $k = M_{12} / \sqrt{L_1L_2}$. For all the calculations,

square coils are used rather than circular because their inductance calculation runs faster (see Appendix 1). The behavior of a circular coil is virtually indistinguishable from a square one with the same area, as Figure 7 shows for the case g/a=0.03. Notice that the curves become negative past x/a ~ 0.6 because the direction of the net flux through the armature reverses, as Figure 8 indicates. Flux reversal does not occur the cylindrical geometry of Figure 1.
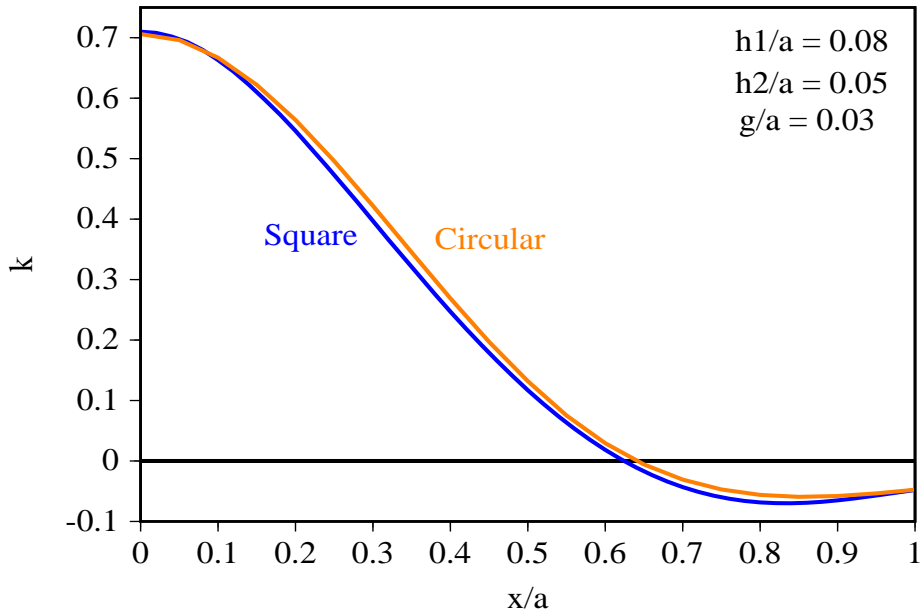

Figure 7. Comparison of the inductive coupling of a circular and square coil of equal area.
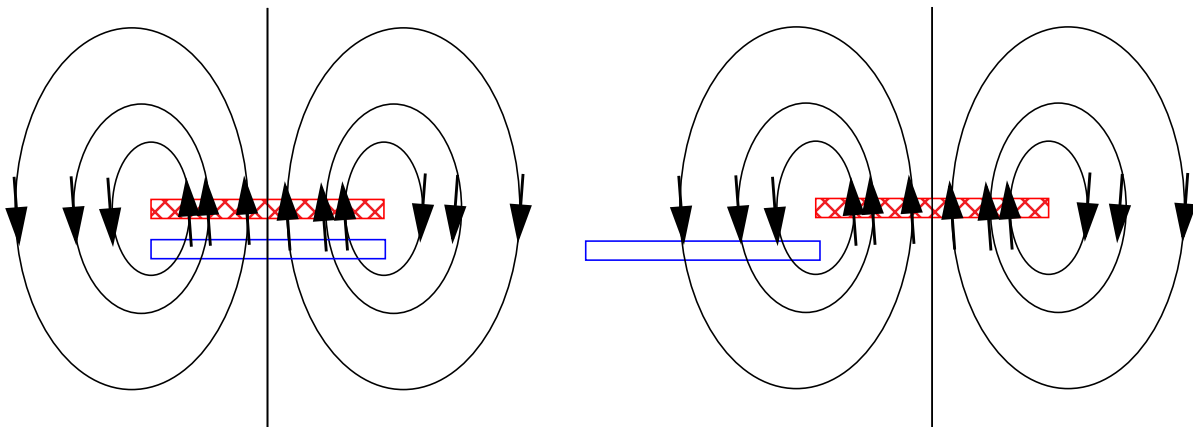

Figure 8. Reason for the coupling sign change. When the passive plate (blue) lies directly below the powered one (red, cross hatched), the flux through it points upward. When it has moved a diameter, the flux points down. Somewhere between (at ~ 0.6 diameter), the net flux vanishes.

The coupling constant for the square coils described above is plotted as a function radial separation in Figure 9 for a number of scaled gaps, g/a. The curve shows both the strength of the current induced in the armature (proportional to M), and the resulting force per unit current (proportional to -dM/dx). The thrust can, therefore, be estimated by the product -MdM/dx, plotted in Figure 10. As expected, smaller gaps produce larger forces. The location of the peak force is also weakly gap dependent.
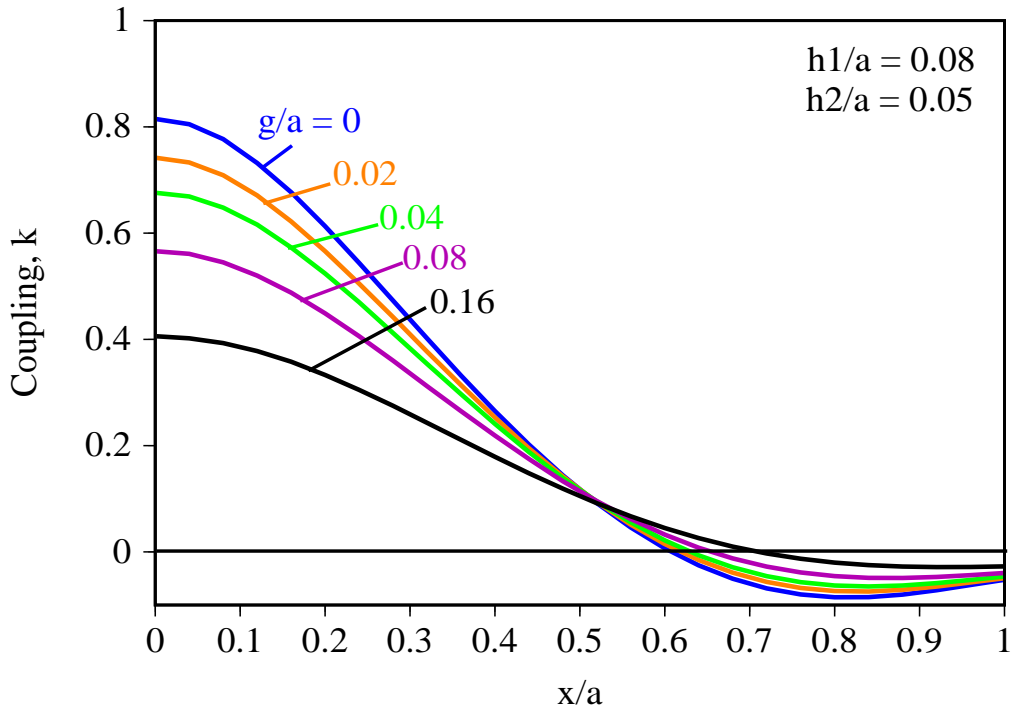
Figure 9. Inductive coupling between square two coils as a function of their separation in the direction of motion for a number of axial gaps. All lengths are scaled to the transverse width, a.
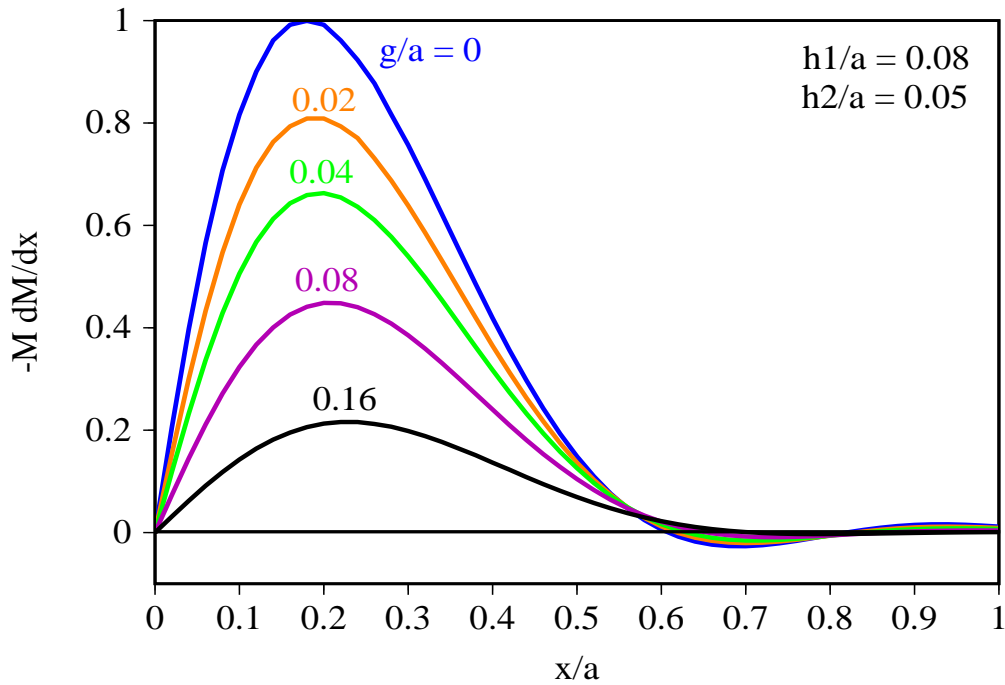

Figure 10. a) Normalized force, -M dM/dx, for square coils as a function of position for various gaps.

V. A benchmark example

Consider a benchmark example in which the powered coil is copper at 100°C while the passive one is aluminum at 30°C. Both have 100 turns and 75% fill fraction. The coils are square: $a = b = 1$ m, and completely filled: $d = 0.5$ m. The powered and passive coil heights are 8 and 5 cm respectively, the gap between them is 3 cm, and the relative velocity is 40 m/s. A sinusoidal 10 kilovolts at 200 Hertz is applied.

Figure 11a plots the applied voltage, V, the powered current, I_1, and the induced current, I_2. Figure 11b gives the horizontal "thrust", F_x, and the vertical" lift", F_z. The average thrust is 10 kNt. Notice that the lift is about 3 times greater than the thrust. Figure 11c shows how the input power, $I_1 V$, is distributed among the various energies. Figure 11d plots the efficiency. Power to the coil would typically be switched off at the current null at 0.5 meters. At this time the inductive energy is zero, the average force is 10 kNt, and the efficiency is 77%. The envelope of the thrust in Figure 11b is essentially the appropriate force profile in Figure 10 modulated at 200 Hertz.
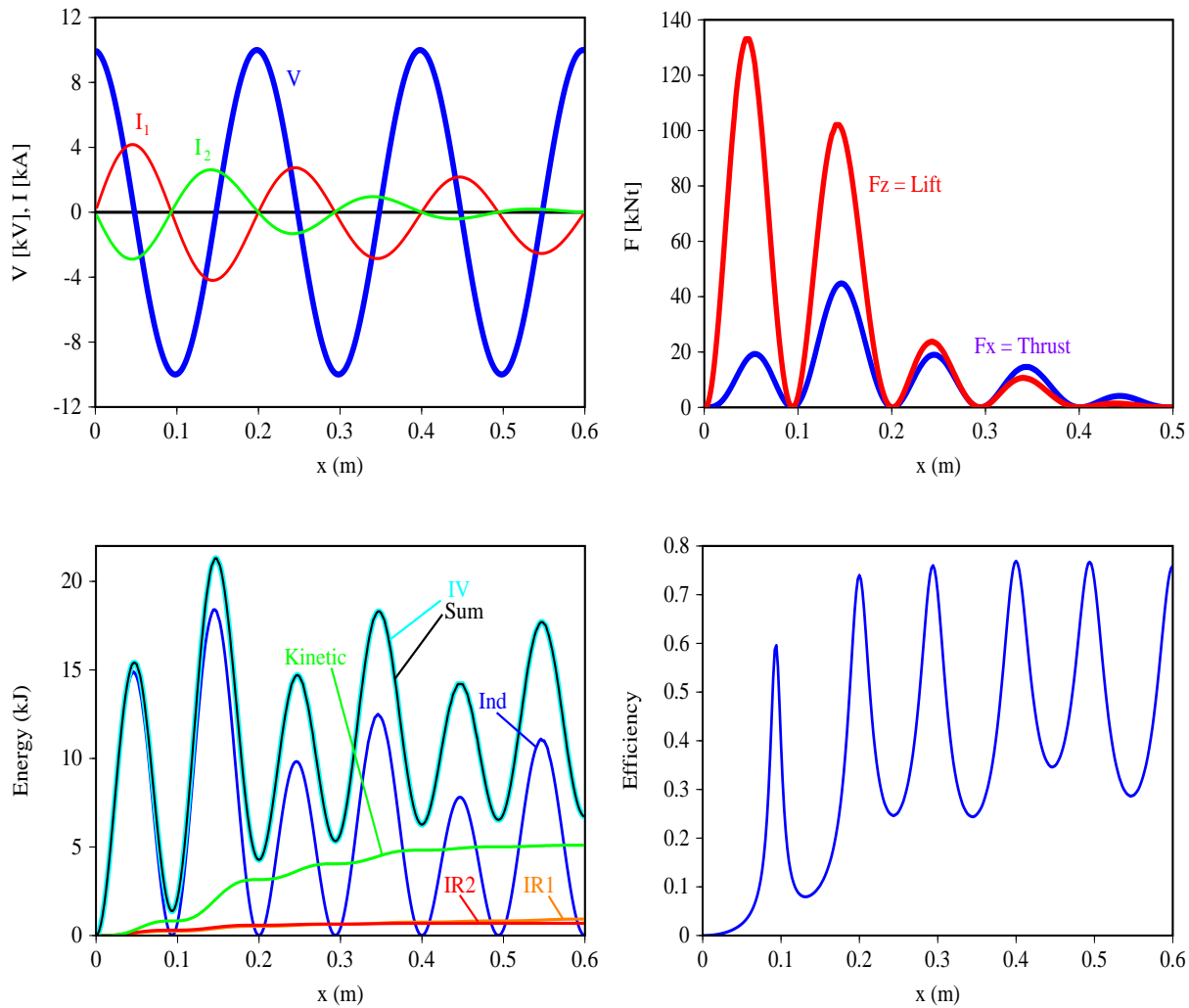

Figure 11. a) Applied voltage and current in both coils. b) The thrust (blue) and lift (red). c) Energy: inductive, ohmic (1&2), and kinetic. The input (integrated IV) and sum should be, and are, equal. d) The efficiency as defined by (5).

When a motor coil is positioned over a track coil so as to produce a force in the desired direction, the alternating current is switched on and maintained as long as it produces significant force. The frequency must be sufficiently high so that switching can occur both near the optimal coil/coil configuration and at a current null to avoid arcing. The higher the peak desired speed, the higher the required frequency. Once this frequency is chosen, however, it remains fixed. Only the duration of the power pulse changes with velocity, not the frequency. For speeds up to about 60 m/s, 200 Hertz is sufficient. It would not be for 100 m/s.

VI. Parameter study

In this section we examine the effects of altering the benchmark parameters. The metrics used to evaluate performance are the voltage necessary to produce an average force of 10 kNt, the peak circulating power, and the efficiency. The only energy sinks in this ideal problem are ohmic and kinetic. The inductive energy, by far the largest component, is recovered after each cycle. In reality, of course, parasitic losses occur as eddy currents that are induced in surrounding conductors lower the efficiency.

Figure 12a illustrates the effect of varying the gap. Increasing the gap increases both the required voltage and circulating power while decreasing the efficiency. While a smaller gap is clearly preferable, the degradation is not precipitous. For example, increasing the gap from 2 to 4 cm only reduces the efficiency from 75% to 73%. Even at 6 cm the efficiency is 71%.

The effect of varying the fill fraction, taken to be the same in both coils, is shown in Figure 12b. Notice that the required voltage and circulating power are virtually unchanged. The circuit behavior is dominated by its large inductance; the resistance is insignificant by comparison. Lowering the fill factor does, however, affect the efficiency by increasing ohmic losses.

Figure 12c gives the result of varying the common coil height, h. Notice that the efficiency increases with h, but so does the voltage and peak inductive power. The efficiency rises because the larger cross-section of the coils reduces the current density, so less energy is lost to ohmic heating. But because the inductive coupling decreases with increasing height, more current, and thus higher voltage, is needed to achieve the same force. High voltage and high circulating power place demands on the power supply. Therefore, the coil height should be big enough for decent efficiency, but small enough to keep the required voltage and circulating inductive power down.

In Figure 12d, the powered coil height, h_1, is 8 cm, while the passive coil height, h_2 varies. When the track coil is too thin, its high resistance hurts the efficiency. When it is too thick, efficiency suffers due to diminished coupling. Although there is an optimal thickness for efficiency around 8 cm, both the voltage and circulating power increase monotonically with h_2.

Figure 12e shows that performance improves in all regards as the winding width, d, increases. The best design is when all the available volume is occupied (d=0.5 m). The worst performance is for a thin hoop (d=0.1 m).

Figure 12f plots the performance for coils as b is reduced, shortening them in the direction of motion. The rationale for doing this is that although the longitudinal segments contribute to the inductive coupling, only the transverse segments produce thrust. To keep the same number of cycles with the shorter coil, the frequency is increased proportionally. For example, for b=20 cm, the frequency is increased to 1000 Hertz. Reducing b increases the voltage and circulating power needed to produce 10 kNt. As the coil becomes shorter, the ratio of the gap to the longitudinal length, g/b, increases, reducing the coupling and adversely affecting the efficiency. Performance would improve if the gap were shrunk proportionally.
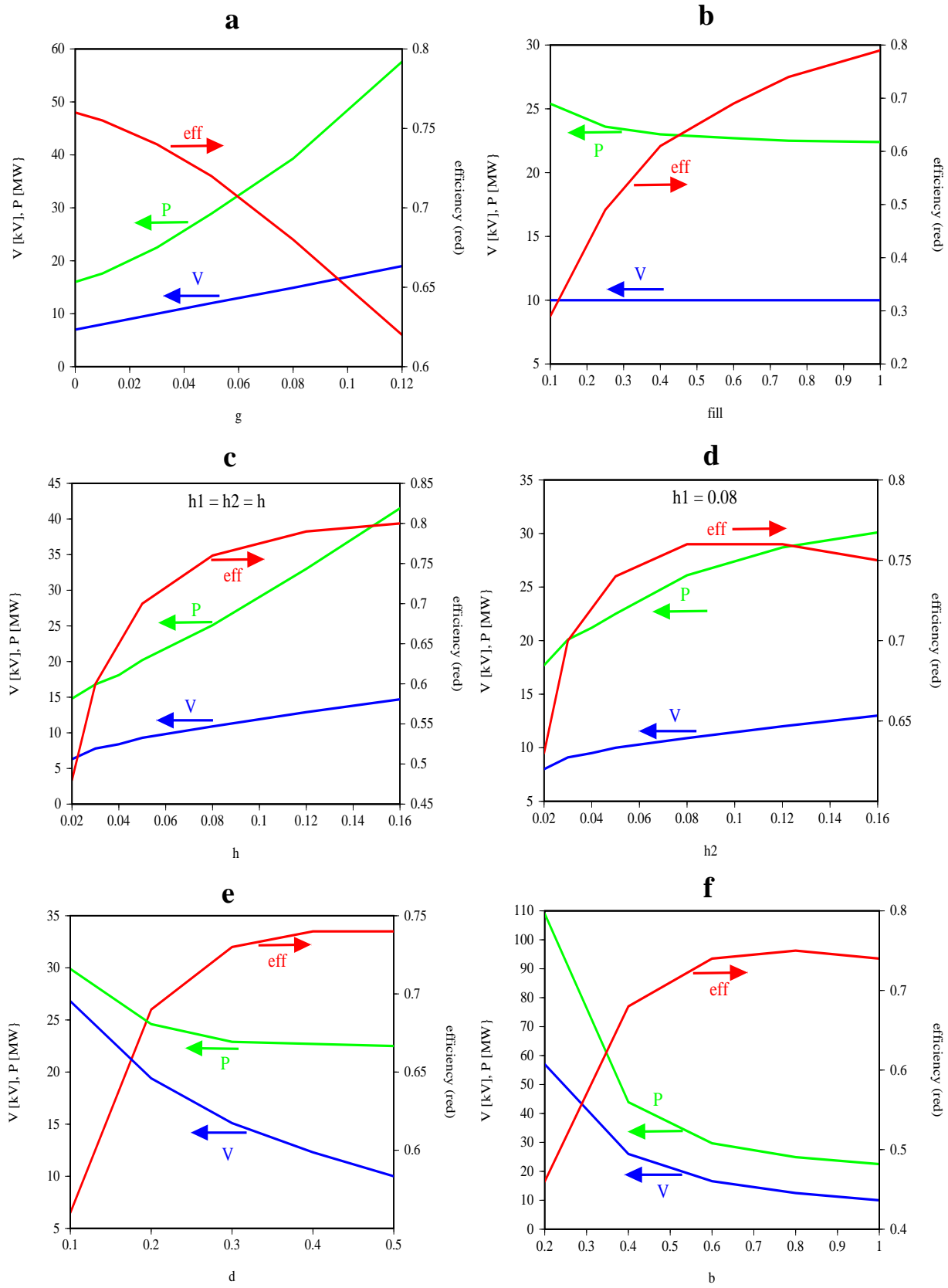
-12-

Figure 12. The required voltage (blue) and peak circulating power (green) are on the left axis, the efficiency (red) is on the right. For an average force of 10 kNt: performance as a function of a) gap, b) fill fraction, c) heights, d) track coil height, e) winding width, and f) aspect ratio.

In addition to the horizontal design in which the track coil lies flat on the roadbed, Figure 13a, there are two symmetric configurations, each with three elements. In the original SERAPHIM concept, Figure 13b, two vertical powered coils straddle a linear array of passive plates (or shorted coils), the "segmented rail". The proof-of-principle demonstration and early studies were based on this design. In the other symmetric configuration, Figure 13c, the powered coil extends vertically downward into a slot in the guideway and the passive elements line both sides. The symmetric designs have better magnetic coupling and produce no lift.

An undesirable feature of the symmetric designs is that, while the two outside coils repel the element between them, they attract each other. This produces a torque which changes with their relative position. This is less of a problem for the single powered coil design because the induced current in the track coils, and the resulting attractive force, is smaller. The magnetic coupling is also better for this design because the two passive coils intersect more of the magnetic flux from the centered powered coil than does the single centered element in the original design. For these reasons, and some engineering considerations, the symmetric single powered coil approach appears superior to the original symmetric concept, even though it does require twice the number of track coils. The improvement of the best symmetric configuration over the single sided one is given in the following table. Again, the average thrust is 10 kNt.

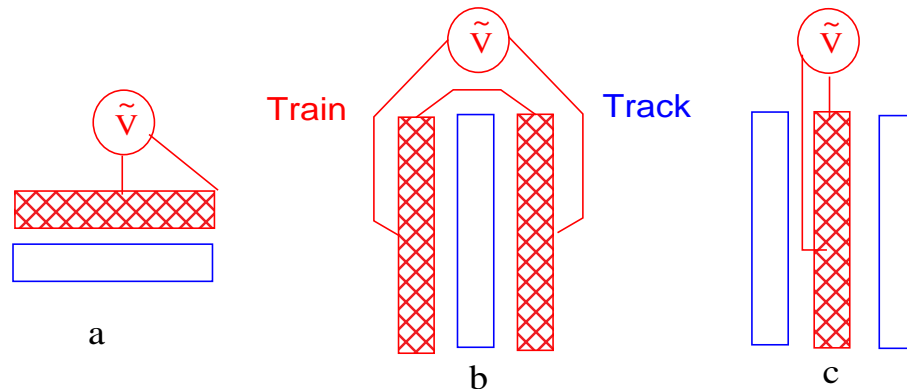|	V(kv)	P(MW)	efficiency
Single sided (Figure 13a):	10.0	23.5	75%
Two sided (Figure 13c):	6.6	14.7	79%

Figure 13. a) Single sided configuration with powered coil (red, cross hatched) above passive, shorted track coil (blue). Symmetric three coil configurations: b) Original concept, c) preferred design with single powered coil between two track coils.

VII. Motor considerations

As shown in Figure 10, the force on a powered coil lasts roughly from the time it is centered over a track coil until its axis crosses the track coil's edge. At this time its power is switched off and it coasts onto the next track coil. Where should this next track coil be? The original concept was to leave a full diameter of space between coils to avoid the retarding force produced as a powered coil slides off the in-play track coil and onto the next track coil. It was soon realized that the vehicle coil only produces force for about half a diameter. This is true even when a solid plate

is used for the track (See Appendix 2). Since the power is switched off after moving half a diameter, it was thought that the next track coil should be placed half a diameter away. As Figure 10 shows, however, the force between coils is so weak when their centers are more than a radius apart, that the coils could actually be placed adjacent to each other, accepting the slight retarding force produced by the overlap with the next track coil during the powered portion. By placing the track coils adjacent to each other rather than separated by a radius, the "duty cycle", the fraction of time the coil is energized, is increased from 1/3 to 1/2. This configuration is illustrated in Figure 14. The performance of separated and adjacent geometries are compared in Figure 15. They are nearly identical except near the end, where the retarding force is felt. The change in efficiency is insignificant, dropping from 75% to 74%, a small price to pay for a 50% increase in the duty cycle.

Switch closes at current null when coils are ~ coaxial

Thrust (and lift) from interaction with center track coil

Slight retarding force from next track coil

Switch opens at current null as force vanishes

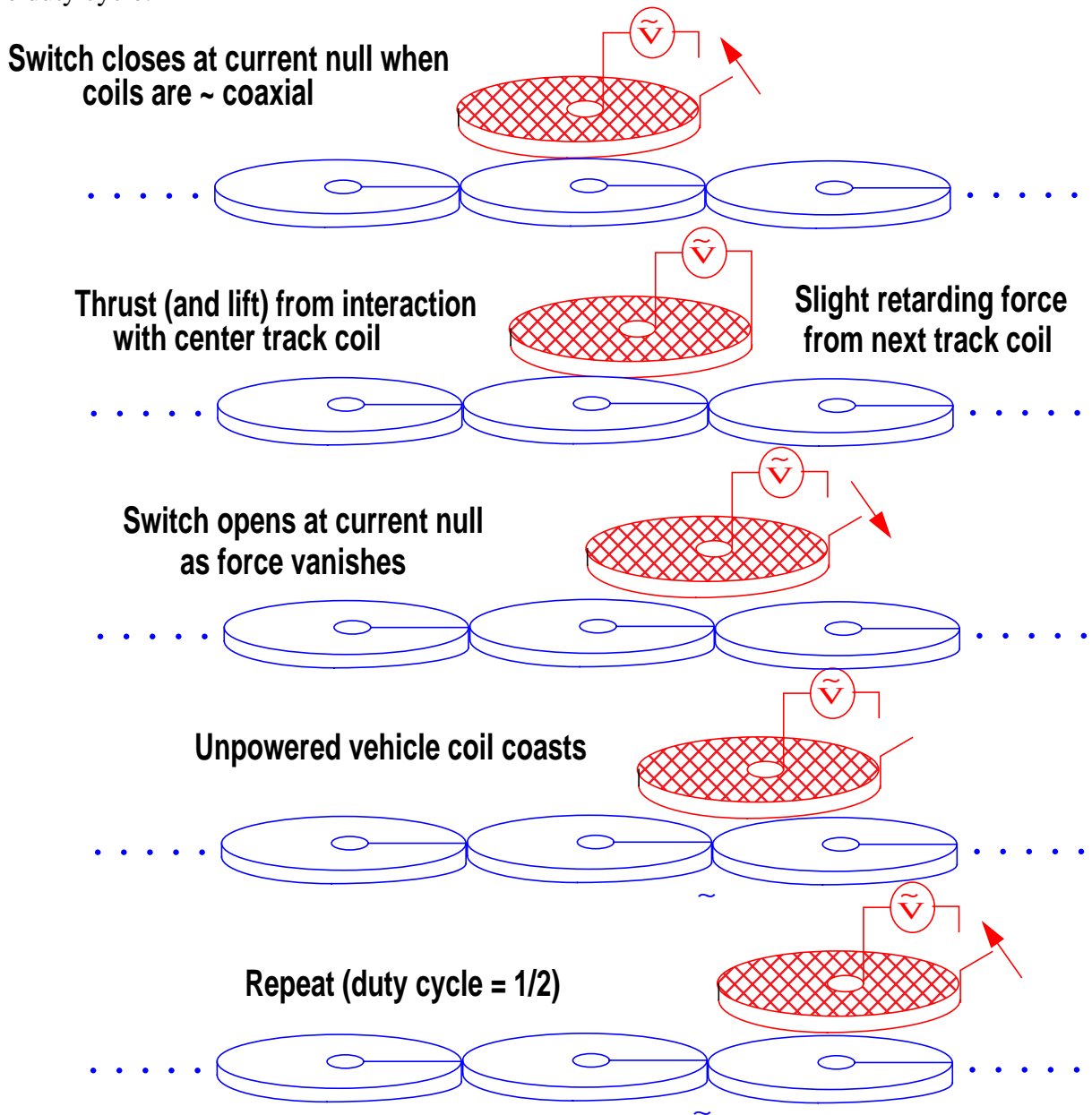**Unpowered vehicle coil coasts**

Repeat (duty cycle = 1/2)

Figure 14. A powered coil (red, cross hatched) moving over adjacent track coils (blue). Small retarding force allows the track coils to be adjacent, rather than half a diameter apart.
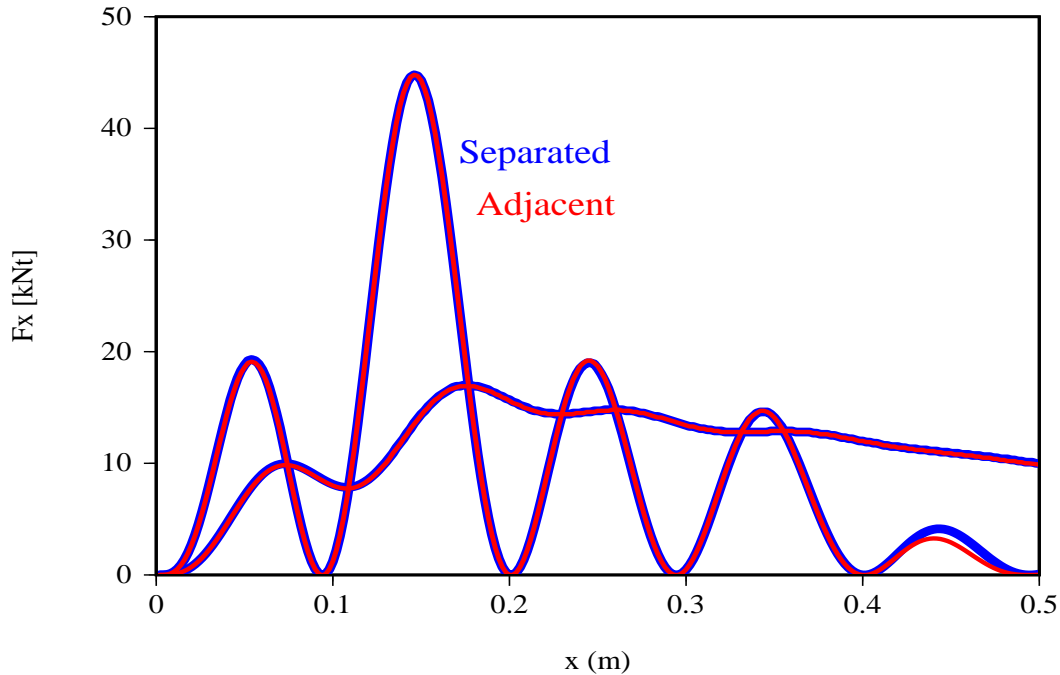
-15-

Figure 15. Instant and average thrust from coils 1/2 diameter apart (blue) and adjacent (red).

A motor based on SERAPHIM technology could have N coils in a line, spaced 1/N diameters apart. That is, if the first coil is directly over a track coil, the offsets would be 0, 1/N, 2/N, ... , (N-1)/N diameters. Figure 16 combines the force envelope from Figure 10 with the firing pattern of several multi-coil motors to yield an average force of 20 kNt. A one coil motor produces a force in a given direction only half the time. Such a motor could function once the vehicle achieves moderate speed. When standing still, however, it may not be able to start in the desired direction. A two coil motor can produce a force in either direction except at the two points when one coil lies directly over a track coil and the other is halfway between two of them. Plus, there will always be a powered coil. With three or more coils, there are no dead spots; at least one coil is always producing a force in either direction. Thus, a minimal practical motor probably has three coils. Where two coils produce force in the same direction, the larger force can be chosen so that only one coil need be active at any time. With four coils, two usually produce a force in either direction. There are, however, positions for which two of the coils exert no force, just as in the two coil case. If the motor happens to stop at one of these spots, only one coil is available to provide force in either direction, and that force is weak. With a five coil motor there are at least two coils, and possibly three, providing force in either direction, one of which is always in a strong position. As before, when three coils are available, the best two can be selected so that there are always two active coils. While more coils produce a smoother force and permit lower stress per coil, they also increase the total size and weight.

A motor consisting of three coils is shown in Figure 17, along with the firing pattern for producing thrust in either direction. A similar diagram is easily constructed for a motor with any number of coils.
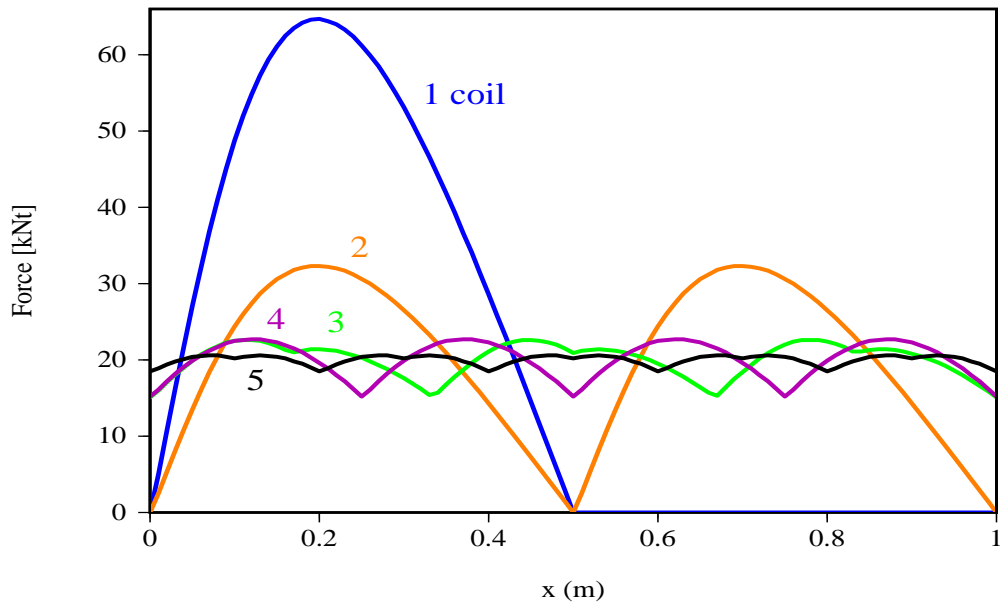
Figure 16. Net force from a motor consisting of 1, 2, 3, 4, and 5 coils. Average force is 20 kNt.
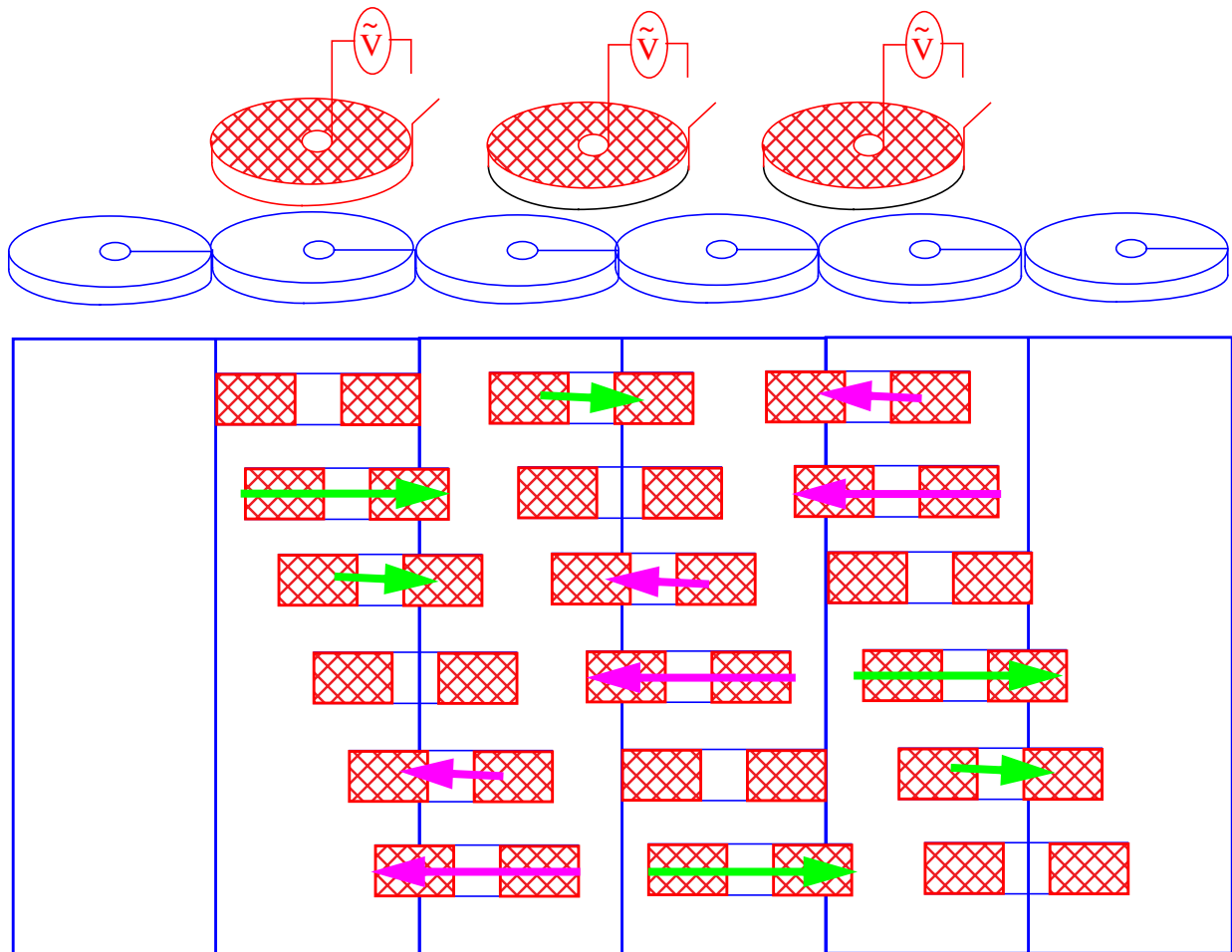

Figure 17. Three motor coils (red, cross hatched) a third of a diameter apart and roadbed (blue). For any position above the track coils, at least one motor coil could provide thrust (green) and one could provide braking (magenta), if its switch is closed.

VIII. Challenges facing SERAPHIM

As of this writing, a motor based on SERAPHIM technology exists only on paper. The single-shot proof-of-principle demonstration, while performing as expected, was not of optimal design and did not include many features essential in a motor suitable for commercialization. A continuously operating motor suitable for integration onto a vehicle must have sensing and control capability. It will need a cooling system to remove the ohmic heat from the powered coil, and shielding to keep the external magnetic fields at acceptable levels (iron shielding might actually improve the electrical performance by increasing the coil inductance!). It will need a power supply to drive the highly inductive load. For example, if the benchmark coil delivers 10 kNt of thrust at 40 m/s, the average power going into kinetic energy is 0.4 MW. As Figure 18 shows, however, although the average circulating inductive power is zero, its peak approaches 25 MW. The coils must be able to withstand repetitive mechanical and thermal stresses. And, of course, the whole package cannot be either too big or too heavy (the copper in the benchmark coil weighs about 400 kg). There will also be issues to consider once the intended use is defined. What is the best way to power the vehicle, an on board engine, power from the grid via a third rail or catenary, or a distributed power generation system? Which is the best geometry, the two coil horizontal design, the three coil symmetric one, or some other configuration? To address these and other issues, an experimental testbed motor is being constructed. Additional parameter studies of systems-level issues are also ongoing.

Ultimately, the question is not whether the motor described here can be built and made to work, but whether it will be demonstrably smaller, lighter, more efficient, and more practical than a LIM, or any other candidate, which delivers the required performance.
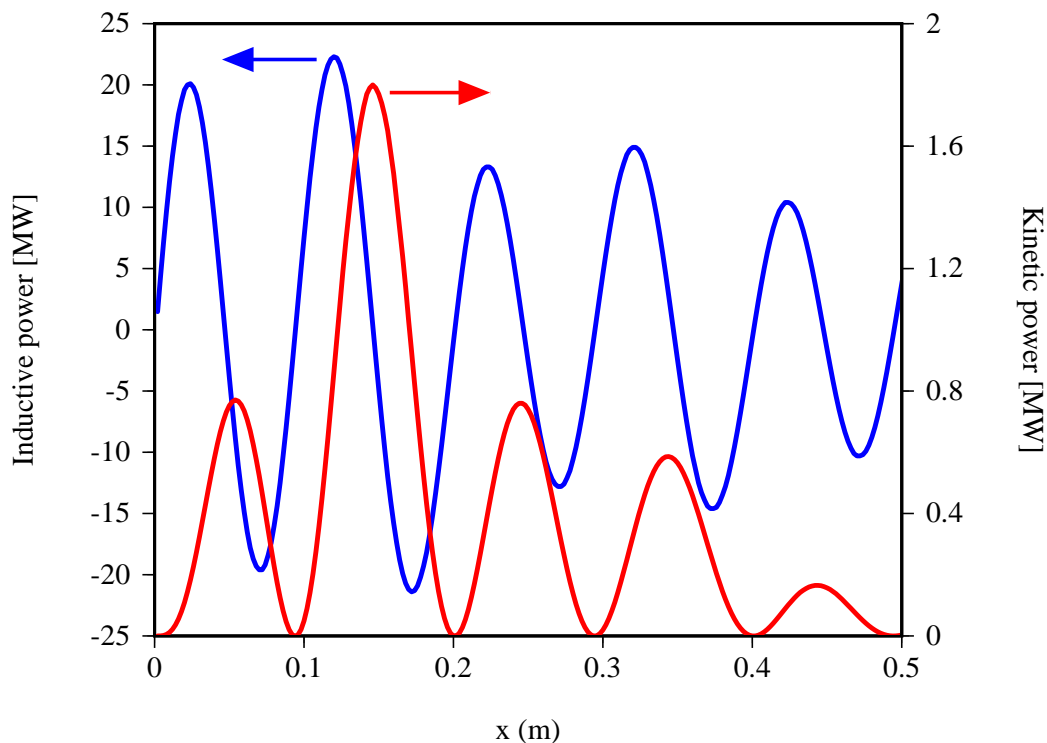

Figure 18. Inductive (blue, left axis) and kinetic (red, right axis) power. Note the different scales.

Appendix 1. Inductance calculations

The self inductance of a circular coil with rectangular cross-section is found from a tabular formula on page 105 of Grover [7]. It involves two parameters, the ratios of the coil width (h) and the winding thickness ($R_{out}-R_{in}$) to the diameter. The data tables (p. 144) are included in the code.

The mutual inductance between two coils is found by replacing each coil by a number of uniformly spaced hoop filaments with parallel axes. The mutual inductance between two hoops of radii r_1 and r_2, and an axial separation of h, and is

$$(A1) \quad M_{12} = \frac{\mu r_1 r_2}{4\pi} \int_0^{2\pi} \int_0^{2\pi} \frac{\cos(\theta_1 - \theta_2)}{r_{12}} d\theta_1 d\theta_2$$

where r_{12} is the distance between points on the two hoops:

$$(A2) \quad r_{12}^2 = (x_2 - x_1)^2 + 2(x_2 - x_1)(r_2\cos\theta_2 - r_1\cos\theta_1) + r_2^2 + r_1^2 + h^2 - 2r_2r_1\cos(\theta_2 - \theta_1)$$

The mutual inductance is found by numerically evaluating the double integral for all pairs of hoops and summing their weighted contributions. M_{12} is a function of the three parameters r_2/r_1, h/r_1, and $(x_2 - x_1)/r_1$. It could be pre-tabulated for faster execution.

The self inductance of a rectangular coil with rectangular cross-section is found by replacing the coil with a number of evenly spaced rectangular circuits. The self inductance of one of these elements is found using an expression on page 60 of Grover for rectangular circuits made from round wire. The diameter used is that which gives it an equal area. The self inductance of the full coil is obtained from a sum of all the self and mutual inductances of the elements.

The mutual inductance of two rectangular coils is found by replacing each with a number of uniformly spaced rectangular filaments with parallel sides, Figure A1. The mutual inductance between two such filaments is found by summing individual contributions from segment pairs:
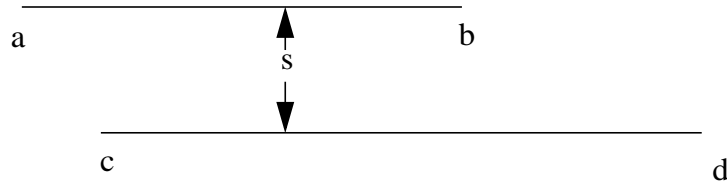

Figure A1. The geometry of two parallel lines used for the inductance calculation.

Evaluating an integral similar to (A1) for these parallel line segments gives

$$(A3) \quad M = 10^{-7} s[f(\alpha) - f(\beta) - f(\gamma) + f(\delta)]$$

where

$$f(x) = x \operatorname{arc sinh} x - \sqrt{1 + x^2} \ , \quad \alpha = \frac{c-b}{s} \ , \quad \beta = \frac{c-a}{s} \ , \quad \gamma = \frac{d-b}{s} \ , \text{ and } \delta = \frac{d-a}{s} .$$

There is no coupling between perpendicular segments. Complicated as these expressions appear, it takes much less computation time to evaluate them than for the double integral of the circular case, for which there is no analytic expression.

Appendix 2. The slotted plate

A solid plate armature does not lend itself to the type circuit analysis performed on the shorted coil. The magnetic field in the plate satisfies a diffusion equation which usually requires solutions for all three components. This can be, and has been, done using finite difference or finite element methods. To the extent that the currents in the plate flow mostly transversely, except at the two ends, the behavior of the solid plate should not be significantly altered by cutting transverse slots in it. If all the elements are thin with respect to the skin depth, the slotted plate can be represented by a parallel circuit consisting of distributed resistances and inductances, as shown in Figure A2. Each of the current loops is inductively coupled to all others and to the powered coil, whose circuit is also shown.

Using a slotted plate with 10 cross pieces, as illustrated, and the benchmark parameters, the behavior with the two different reaction elements can be compared. The inductive couplings of the two geometries, the forces, and the efficiencies are compared in Figure A3. The force distribution with the slotted plate is different and persists somewhat longer. The efficiency of the slotted plate design, however, is lower than the coil because of the high ohmic heating loss on the front edge. This makes both the slotted and solid plate less attractive.
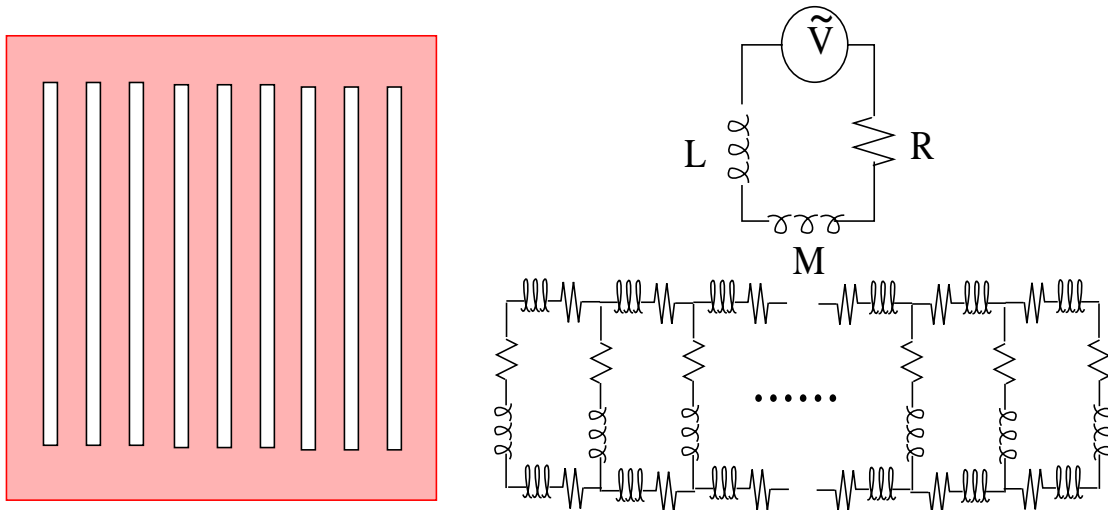

Figure A2. A slotted reaction plate composed of 10 parallel segments and connecting bars top and bottom (left). Its circuit and powered coil circuit (right).
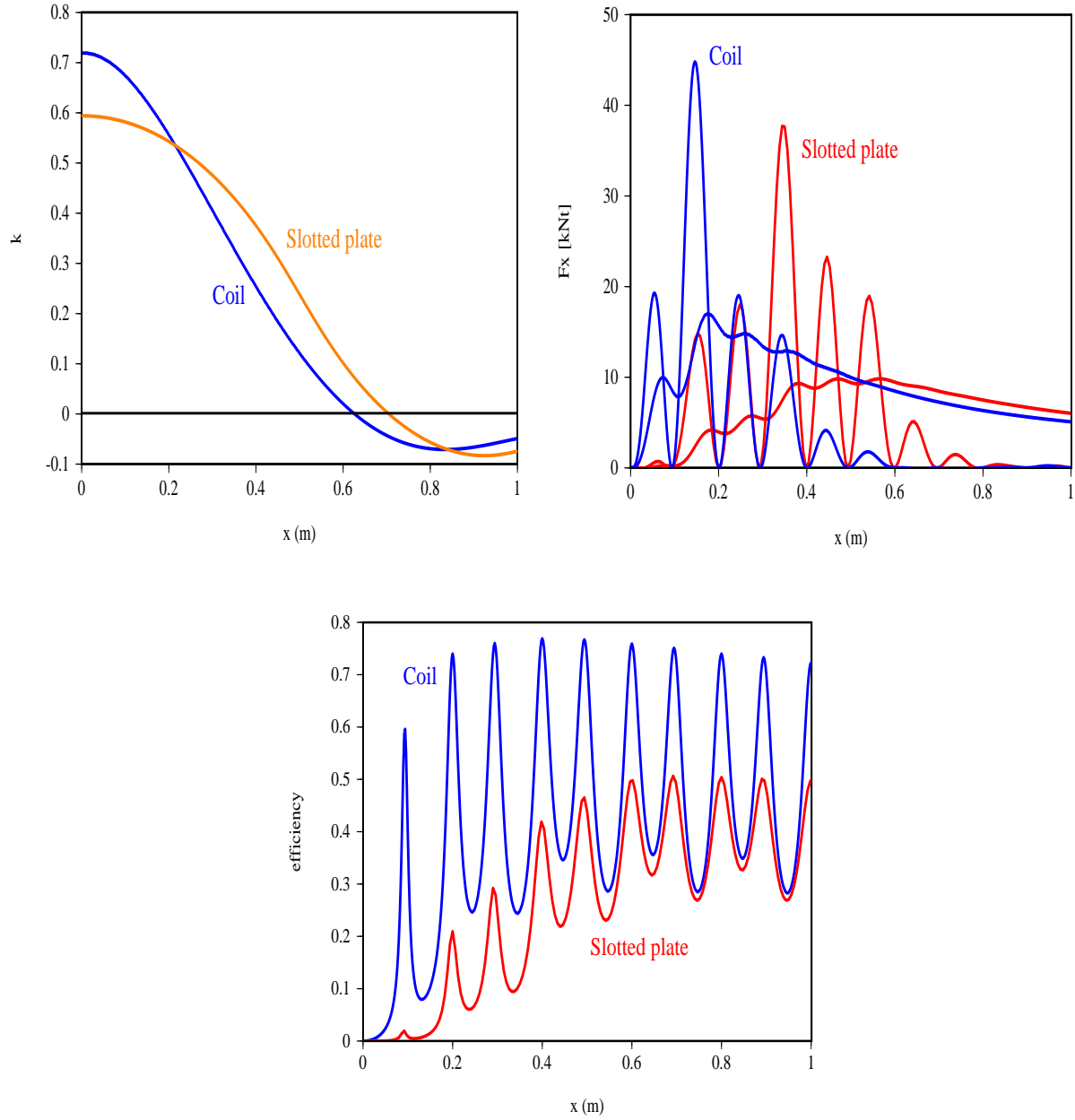
Figure A3. a) Inductive coupling between two coils (blue) and a coil and slotted plate (red) as a function of their centerline separation. b) Instant and average thrust. c) Efficiencies.

References

[1] Jean-Claude Raoul, "How High Speed Trains Make Tracks," *Scientific American,* October, 1997.

[2] G. O. D'Sena, J. E. Leney, "Linear Induction Motor Research Vehicle Speed Upgrading Tests," United States Department of Transportation Report No. 72-8857, June 1973.

[3] MNI Staff, "Final Report on the National Maglev Initiative," Report DOT/FRA/NMI-93/03, September, 1993.

[4] R. J. Kaye, E. L. Brawley, B. W. Duggin, E. C. Cnare, D. C. Rovang, and M. W. Widner, "Design and Performance of a Multi-Stage Cylindrical Reconnection Launcher," IEEE Transactions on Magnetics, MAG-22, 1986.

[5] M. Cowan, E. C. Cnare, B. W. Duggin, R. J. Kaye, and T. J. Tucker, "The Reconnection Gun," IEEE Transactions on Magnetics, Vol 27, No. 1, January, 1991.

[6] B. N. Turman, B, M. Marder, G. J. Rohwein, D. P. Aeschliman, J. B. Kelley, M. Cowan, and R. M. Zimmerman, "The Pulsed Linear Induction Motor Concept for High-Speed Trains," Sandia National Laboratories report SAND-1268, June 1995.

[7] F. W. Grover, <u>Inductance Calculations</u>, Dover Publications, Inc., 1946